**Atmospheric
Chemistry
and Physics
Discussions**

ACPD

10, 6641–6679, 2010

FAME-08

M. Pikridas et al.

Title Page

Abstract	Introduction
Conclusions	References
Tables	Figures

◄◄   ►►

◄   ►

Back   Close

Full Screen / Esc

Printer-friendly Version

Interactive Discussion

The Finokalia Aerosol Measurement Experiment – 2008 (FAME-08): an overview

M. Pikridas[1,2], A. Bougiatioti[3], L. Hildebrandt[4], G. J. Engelhart[4],
E. Kostenidou[1,2], C. Mohr[5], A. S. H. Prevot[5], G. Kouvarakis[3], P. Zarmpas[3],
J. F. Burkhart[6], B.-H. Lee[4], M. Psichoudaki[1,2], N. Mihalopoulos[3], C. Pilinis[7],
A. Stohl[6], U. Baltensperger[5], M. Kulmala[8], and S. N. Pandis[1,2,4]

[1]Department of Chemical Engineering, University of Patras, Greece
[2]Institute of Chemical Engineering and High Temperatures (ICE-HT), FORTH, Patras, Greece
[3]Department of Chemistry, University of Crete, Greece
[4]Center for Atmospheric Particle Studies, Carnegie Mellon University, Pittsburgh, USA
[5]Paul Scherrer Institut, Laboratory of Atmospheric Chemistry, Villigen, Switzerland
[6]Norwegian Institute for Air Research, Kjeller, Norway

[7] Department of Environment, University of the Aegean, Mytilene, Greece
[8] Department of Physics, University of Helsinki, Helsinki, Finland

Correspondence to: S. N. Pandis (spyros@andrew.cmu.edu)

Title Page

Abstract | Introduction

Conclusions | References

Tables | Figures

◄◄ | ►►

◄ | ►

Back | Close

Full Screen / Esc

Printer-friendly Version

Interactive Discussion

M. Pikridas et al.

Abstract

A month (4 May to 8 June 2008) of ambient aerosol, air ion and gas phase sampling (Finokalia Aerosol Measurement Experiment 2008, FAME-08) was conducted at Finokalia, on the island of Crete, Greece. The purpose of the study was to characterize the physical and chemical properties of aged aerosol and to investigate new particle formation. Measurements included aerosol and air ion size distributions, size-resolved chemical composition, organic aerosol thermal volatility, water uptake and particle optical properties (light scattering and absorption). Statistical analysis of the aerosol mass concentration variations revealed the absence of diurnal patterns suggesting the lack of strong local sources. Sulfates accounted for approximately half of the particulate matter less than 1 micrometer in diameter (PM_1) and organics for 26%. The PM_1 organic aerosol fraction was highly oxidized with 80% water soluble. The supermicrometer particles were dominated by crustal components (50%), sea salt (24%) and nitrates (16%). The organic carbon to elemental carbon (OC/EC) ratio correlated with ozone measurements but with a one-day lag. The average OC/EC ratio for the study period was equal to 5.4. For three days air masses from North Africa resulted in a 6-fold increase of particulate matter less than 10 micrometers in diameter (PM_{10}) and a decrease of the OC/EC ratio by a factor of 2. Back trajectory analysis, based on FLEXPART footprint plots, identified five source regions (Athens, Greece, Africa, other continental and marine), each of which influenced the PM_1 aerosol composition and properties. Marine air masses had the lowest PM_1 concentrations and air masses from the Balkans, Turkey and Eastern Europe the highest.

1 Introduction

Elevated particulate matter (PM) concentrations have been related with increased mortality (Pope et al., 1991, 2009). Fine particles with diameter smaller than 2.5 µm ($PM_{2.5}$) are mainly responsible for this association (Pope et al., 2009; Schwartz et al., 1996;

Wang et al., 2008). PM is also linked with climate change because of the particles' ability to scatter and absorb light and to act as cloud condensation nuclei (CCN) thus significantly affecting the earth's albedo (Twomey, 1977; Albrecht, 1989; Lohmann and Feichter, 2005).

Even though the importance of PM has been recognized for several decades, there are still significant gaps in our understanding of its sources and atmospheric transformations. It is well established that gaseous sulfuric acid plays a central role in atmospheric nucleation (Kulmala and Kerminen, 2008), but it alone cannot account for the observed nucleation rates in sulfur poor environments (Kulmala et al., 2004; Stanier et al., 2004a). The hygroscopicity of inorganic salts has been investigated extensively but our knowledge of the water uptake of particles consisting of organic-inorganic mixtures is still incomplete (Cruz and Pandis, 2000; Dick et al, 2000; Meyer et al, 2009). Semi-volatile organic compounds (primary or secondary) partition between the gas and particulate phases. Understanding the partitioning of these organic compounds has been recognized as one of the major challenges in our efforts to quantify the rates of formation of secondary organic particulate matter (Robinson et al., 2007). There is little information about the volatility of these organic compounds especially as the aerosol ages in the atmosphere (Kanakidou et al., 2005; Hallquist et al., 2009). As a part of the EUCAARI (Kulmala et al., 2009) project the Finokalia Aerosol Measurement Experiment 2008 (FAME-08) was designed to address the above issues by collecting measurements of ultrafine, fine and coarse particles, by monitoring water uptake, size resolved PM composition and size resolved volatility of aged organic aerosol that was transported to Crete from Europe, Asia and Africa.

The Eastern Mediterranean basin is a good area for the investigation of the properties of aged PM (Mihalopoulos et al., 1997; Sciare et al., 2003a; Gerasopoulos et al., 2006). The three major sources of PM in the area are particles and their gaseous precursors from industrialized areas in the Balkans and Eastern Europe (Sciare et al. 2003a, b), Saharan dust transported from the south (Moulin et al., 1998; Kalivitis et al., 2007), and sea spray (Koulouri et al., 2008; Kouvarakis et a., 2002; Sciare et al., 2003b;

2008). Long range transport from Europe contributes significantly to non-sea-salt sulfate (Sciare et al., 2003a) with biogenic emissions of marine origin being the second most important contributor (Mihalopoulos et al., 1997; Kouvarakis et al., 2002;).

The majority of aerosol studies in the eastern Mediterranean are focused on megacities such as Athens (Bartzis et al., 2004) and not on remote areas. Few attempts have been made to characterize the PM size distribution away from the urban centers (Lazaridis et al., 2008; Eleftheriadis et al., 2006; Kalivitis et al., 2008) and even fewer to link composition with size (Kavouras and Stephanou, 2002; Schneider et al., 2004; Koulouri et al., 2008). Particle formation has been investigated but without any instrumentation to monitor particles below 10 nm (Kalivitis et al., 2008). There is almost no information about the water uptake of PM in the area.

FAME-08 combined filter-based methods with continuous measurements of number distribution and chemical composition including water in order to assess the physical, chemical and optical properties of "aged" PM. In this overview paper we briefly describe the full set of measurements of FAME-08 with experimental procedures described in Sect. 4. In Sect. 5 there is an overview of the experimental results including analysis of the diurnal patterns of the various pollutants and analysis of source regions affecting the site during the measurement period. A synthesis of the results is presented in Sect. 6.

2 Site description

Finokalia (35° 24′ N, 25° 60′ E) is a remote coastal station located in the southeast of the Mediterranean Sea on the island of Crete, Greece (Fig. 1). The nearest large urban center is Heraklion with 150 000 inhabitants located 50 km west of Finokalia. The Finokalia station is located at the top of a hill at an elevation of 230 m facing the sea. There is no notable human activity at a range of approximately 15 km (Kouvarakis et al., 2000).

3   Program objectives

FAME-08 was designed in order to improve our understanding of the physical, chemical and optical properties of aged European aerosol as it is transported from central to southeastern Europe. Its objectives were:

5 1. Characterization of the PM size, surface area, volume distribution and its physicochemical properties.

2. Characterization of PM chemical composition as a function of size.

3. Improved understanding of the mechanisms of in-situ formation of particles in this area.

10 4. Quantification of the role of organic matter in the water uptake by PM as a function of aerosol age.

5. Linking the volatility of PM with age, sources, and source areas.

4   FAME-08 measurements

FAME-08 was conducted from 4 May to 8 June 2008 and provided continuous mea-
15 surements of physical and chemical characteristics of PM, air ions, gaseous species and meteorological parameters. The frequency, resolution and the exact operation period of each method are summarized in Table 1.

PM inorganic components: A custom made virtual impactor (Loo and Cork, 1988) was used to collect particles with diameters less than 1.3 µm ($PM_{1.3}$) and particles with
20 diameters between 1.3 and 10 µm ($PM_{1.3-10}$) daily on Teflon filters (Millipore, Fluoro-pore membrane filters of 3.0 µm pore size). All collected filters were divided in half and extracted in ultrasonic bath with 20 ml of nanopure water for 45 min for the determination of water soluble ion (Koulouri et al., 2008). For the analysis of anions a Dionex

AS4A-SC column was used, with isocratic elution at 2.0 ml min^{-1} of Na$_2$CO$_3$/NaHCO$_3$ as eluent. For the analysis of organic anions, an AS11 analytical column was used, with NaOH (0.1–3.5 mM) as eluent in a gradient mode. For the analysis of cations a CS12-SC column was used, under isocratic conditions with 20 mM MSA eluent and flow rate of 1.0 ml min^{-1}. All ion species were detected by conductivity detectors. PM$_1$ inorganic components were also monitored by a Quadrupole- Aerosol Mass Spectrometer with details provided below.

The PM$_{1.3-10}$ filters were also analyzed for trace metals. An acid microwave digestion procedure followed by Inductively Coupled Plasma Mass Spectrometry (ICP-MS, Thermo Electron X Series) was applied to measure concentrations of Al, Ca, Ti, V, Cr, Mn, Fe, Ni, Cu, Zn, Cd and Pb (Koulouri et al., 2008). The digestion procedure was performed in Teflon vessels (DAP – 60 K, 60 ml/40 bar) in a microwave digestion system (Berghof MWS – 2). An internal standard (In, CPI International, S4400-1000241) was added to the digested samples before the ICP-MS analysis (Koulouri et al., 2008).

PM$_{2.5}$ semi-continuous measurements of water soluble inorganic ions were conducted by a steam sampler-ion chromatograph at a flow rate of 16.7 Lpm. The system consisted of three parts: (1) a set of annular diffusion denuders (URG-2000) to remove water soluble gaseous species (e.g. NH$_3$, SO$_2$, HNO$_3$), (2) a steam-jet aerosol collector (Khlystov et al., 1995) and (3) two ion chromatographs (IC's) (Metrohm 761 Compact IC) for quantitative mass analysis of anions and cations respectively. A LiF solution of known concentration was mixed with the sample at a flow of 0.1 ml min^{-1} prior to analysis, as an internal standard. The cations and anions IC were equipped with 1000-μl and 200-μl sample loops respectively.

Aerosol Mass Spectrometry: A Quadrupole Aerosol Mass Spectrometer (Q-AMS) from Aerodyne, Inc. was used to measure non-refractory (NR) PM$_1$ chemical composition semi-continuously (Jayne et al., 2000; Jimenez et al., 2003). The instrument determined the size distributions of sulfate, nitrate, chloride, ammonium, water and organics. The calibration of the instrument is described by Hildebrandt et al. (2010). Applying the Kostenidou et al. (2007) algorithm, a total collection efficiency factor (CE)

was estimated for the AMS for every two hours. The average CE for the ambient PM during the campaign was equal to 0.85. A more detailed description of the CE analysis can be found in Lee et al. (2010).

PM carbonaceous material: PM_1 was collected on quartz fiber filters (Whatman QMA, 1851-047), on a daily basis using a custom-built sampler described by Saarikoski et al. (2008). PM_1 organic and elemental carbon (OC and EC) was measured using a modification of the NIOSH thermal–optical transmission method, using a carbon analyzer (Sunset Laboratory Inc., Oregon). The method has two distinct phases to differentiate between OC and EC. During the first phase (OC phase) the sample is kept in a helium atmosphere and heated in four steps, reaching 650 °C, while the second phase (oxygen or EC phase) has two consecutive temperature steps, reaching 850 °C. Ambient and thermally denuded organic aerosol was also monitored by the Q-AMS (Hildebrandt et al., 2010).

Water soluble organic carbon (WSOC) was measured daily using a Shimadzu V_{CSH} Total Organic Carbon (TOC) analyzer and PM_1 filters (Whatman QMA, 1851-047). A punch of $1\,cm^2$ was extracted with 15 ml of nanopure water for 45 min, filtered (Ion Chrom Acrodisc 13, 0.45 µm) for the retention of the non-soluble species and analyzed with the TOC (Sciare et al., 2008). All soluble carbon containing compounds in the solution were oxidized to form carbon dioxide, which was then measured by a non-dispersive infrared (NDIR) gas analyzer. Next, the inorganic carbon was measured, by acidifying the sample and converting all the carbonates, hydrogen carbonates and dissolved carbon dioxide to carbon dioxide, which was volatilized by bubbling air through the sample. The produced carbon dioxide was also measured by the NDIR. The water-soluble organic carbon is the difference between the total and inorganic carbon.

Organic aerosol volatility: The volatility of the organic aerosol was measured using a thermodenuder system built based on the design of An et al. (2007). The aerosol flow was directed alternately, via a system of solenoid valves, either through the thermodenuder (set at a predefined temperature) or through a bypass line. In order to avoid recondensation of organic vapors, activated charcoal (4–14 mesh, Sigma Aldrich) was

used in the cooling stage. At the end of the thermodenuder, the aerosol path was split in two lines and particles were sent to a Scanning Mobility Particle Sizer (SMPS) and the Q-AMS for real-time measurement of the aerosol size distribution and chemical composition respectively. The volatility was then determined by comparing the residual aerosol after the thermodenuder to the aerosol that was passed through the bypass (Lee et al., 2010).

Number distribution: The PM size distributions were monitored by:

(1) An Air Ion Spectrometer (AIS) which monitored ions in the range of 0.8 to 40 nm (Mirme et al., 2007);

(2) Two standard SMPS systems (TSI 3936L, TSI 3034) that monitored fine PM in the size range of 10 nm to 500 nm. The TSI 3034 SMPS monitored the size distribution of ambient and thermally denuded particles in sequence in a temperature controlled environment, while the TSI 3936L was part of the Dry-Ambient Aerosol Size Spectrometer (DAASS) which alternately monitored the distribution of ambient and dried (RH<30%) aerosols at ambient temperature (Stanier et al., 2004b).

PM water and hygroscopicity: The ability of ambient fine particles to absorb water and grow was measured using the Dry-Ambient Aerosol Size Spectrometer (DAASS), (Stanier et al., 2004b). The aerosol path was alternated, via a system of solenoid valves, between the low relative humidity (RH) and ambient conditions. Low RH (<30%) was achieved by sampling ambient air through a system of Nafion dryers prior to measurement by an SMPS (TSI 3936L). The water content of aerosols from 10 nm to 500 nm was computed as the difference in particle volume distributions at ambient RH and at low RH (Khlystov et al., 2005). The DAASS was kept at ambient temperature under a weatherproof sunshade. A fan was employed to ensure constant circulation of ambient air around the instruments.

PM optical properties. Aerosol absorption was monitored continuously by two instruments: a Magee Scientific Aethalometer (Model AE-20) and a Particle Soot Absorption Photometer (Radiance Research) operated at 3 wavelengths. Two nephelometers (Radiance Research Integrating Nephelometer, Model M903) were also used connected in

series by a diffusion drier. These two nephelometers were kept under a weatherproof sunshade in order to ensure that operation was under ambient temperature and RH. Temperature and RH were measured at the inlet of each instrument. The first nephelometer measured the scattering coefficient at ambient conditions and the second at low RH. A third nephelometer (TSI Model 3563) measured the scattering coefficient at three wavelengths in a controlled environment.

Gaseous species: Continuous measurements of O_3 by two instruments (Thermo Electron Model 49C, Dasibi Model 1008 RS) and CO (Thermo Electron Model 48C) using high-sensitivity gas analyzers were conducted. Glass fiber filters (GFF Whatman, 1822047) were soaked in a citric acid-glycerol solution, for the measurement of gas-phase NH_3 and paper filters (Whatman, 1441047) were soaked in sodium carbonate/glycerol solution, for the measurement of gaseous acids (HCl, H_2SO_4, HNO_3). These filters were downstream of bulk PM collecting filters (Millipore Fluoropore membrane filters, 0.45 µm) and were replaced every six hours.

Meteorology: Temperature and relative humidity (MP101A Humidity-Temperature, ROTRONIC), wind speed and direction (05103 Wind Monitor, NovaLynx Corporation), and UV intensity (Pyranometer CM3, Kipp & Zonen) were monitored with a 5 min resolution throughout the campaign.

A source region analysis was conducted and the categories used were named by the region from which the air originated: Marine, Africa, Greece, other continental and Athens. Athens was separated from Greece in order to investigate whether the effect of this megacity could be detected at the field site, about 400 km away. We categorized the air masses based on their source region using the footprint potential emission sensitivity (PES) from 20-day retroplume calculations with the particle dispersion model FLEXPART in backward mode (Stohl et al., 2005), with three hour resolution. Additional information about PES calculations can be found in Seibert and Frank (2004). A retroplume was attributed to a region if that region had a PES value above 0.9 ns kg^{-1}. For periods in which more than one source region had PES values above the threshold, we attributed that air mass to that region which had the larger area with PES value

above the threshold. In order to characterize a retroplume as marine, all PES values above $0.9\,\mathrm{ns\,kg^{-1}}$ had to be located either over sea or over the island of Crete. The marine aerosol that passed over Crete before reaching the field site was not significantly different in composition from the aerosol that was strictly marine and therefore the two were lumped together. A retroplume was characterized as other continental if it was associated with west Turkey or the central and northern Balkans.

5   Overview of measurements

5.1   Statistical analysis

For the source region analysis two statistical tests were employed. First, one-way analysis of variance (ANOVA) was employed to reveal if any of the source region contributions had statistically significant differences, at the 99% confidence level (α=0.01), compared to the rest. If the ANOVA test showed that such a difference existed then the Tukey-Kramer test was employed for every possible combination of source regions at a confidence level of 99%. Unlike ANOVA, which can only be used to look for at least one different pair among a group without being able to indicate which pair is different, the Tukey-Kramer test can indicate which differences between pairs of groups are significant at a given confidence level, for an uneven dataset and without confidence loss (Wheater and Cook, 2000). The ANOVA test was also employed to find if statistically significant diurnal variation existed at the 95% confidence level (Hildebrandt et al., 2010).

5.2   Source region analysis

Marine aerosol that passed over Crete before reaching the field site had a similar composition as the aerosol that did not pass over Crete. This fact suggests that the local, Cretan sources, influencing the field site are not significant and that the marine aerosols are affected by the naval activity of the Mediterranean.

The origins of the air masses reaching the sampling site during the experiment are given in Fig. 2. The PM concentrations and meteorological conditions grouped by source region are shown in Table 2.

Air mass origin was related to local temperature and relative humidity only in the case of Africa. Average temperature was on average 4 ˚C higher and relative humidity was on average 16% lower for this period due to the hot and dry air masses originating from Africa.

PM_1 sulfate concentrations were statistically different among all source regions at the 99% level. Air masses passing over Athens resulted in the highest PM_1 sulfate ($7.5\pm2.2\,\mu g\,m^{-3}$), followed by Greece (6.8 ± 3.0), other continental ($5.9\pm2.8\,\mu g\,m^{-3}$), African ($5.0\pm1.7\,\mu g\,m^{-3}$) and marine air masses ($3.0\pm1.3\,\mu g\,m^{-3}$). The significance of sulfate long-range transport to the area of Finokalia is quite evident from these results as well as the influence of Athens to the site. PM_1 ammonium in marine air masses was statistically lower ($1.0\pm0.4\,\mu g\,m^{-3}$) than that from the other source regions ($>1.7\,\mu g\,m^{-3}$). PM_1 nitrate concentrations were low during the study (less than $0.1\,\mu g\,m^{-3}$ on average) and were statistically similar for air masses coming from Athens, Greece, other continental and marine source regions. There was a statistically significant increase of PM_1 nitrate for African air masses which may be attributed to the increased nitrate content of dust although it is mostly of supermicron size. Acidity of PM_1, defined here as the ratio of AMS ammonium to sulfate (in molar equivalents), was statistically equal for African, marine and other continental source regions but was significantly higher for Greece and Athens ($\alpha = 0.01$).

Organic aerosol in air masses from Athens and other continental origin ($3.2\pm1.0\,\mu g\,m^{-3}$) was statistically higher than that from Greece ($2.6\pm0.7\,\mu g\,m^{-3}$). Organic aerosol contributions were statistically smaller when they originated from Africa ($2.1\pm0.8\,\mu g\,m^{-3}$) and marine areas ($1.9\pm0.8\,\mu g\,m^{-3}$).

Number concentrations of air masses from Athens, Greece and of other continental origin were statistically the same but higher by 25% than those of marine and African origin. Air ions below 2 nm followed by AIS were statistically similar for all source

regions ($\approx$520±150 cm^{-3}), with the exception of Africa (662±225 cm^{-3}) which was sta-
tistically higher. Aerosol absorption (522 nm) was higher for aerosols originating from
Africa (8.5±3.4 Mm^{-1}) than for all other source regions. This is probably due both
to the increased EC concentrations measured during that period and to the high dust
5 levels which can also absorb radiation. Lower absorption was found for air masses
originating from Athens and other continental source regions (5.7±1.6 Mm^{-1}).

5.3 Meteorology

The daily and diurnal variations of meteorological variables are shown in Figs. 3 and 4
respectively. All diurnal profiles are given with respect to local standard time (UTC+2).
10 The lowest ambient temperature at the site was 12 °C and the highest 30.5 °C while
the average temperature was 20°C. The average daily ambient temperature increased
during the study as we moved from late spring to early summer (Fig. 3a). The maximum
temperature occurred in the afternoon (2–5 p.m.) and the minimum in the late night (3–
6 a.m.).
15   Relative humidity varied greatly (Fig. 3b) having an average value for the study equal
to 63%, with a minimum of 18% and a maximum of 99.8%. The diurnal profile of relative
humidity had no statistically significant variation at the 95% confidence level (Fig. 4b).
During FAME-08 solar radiation was intense reaching a maximum value of 1049 W
m^{-2}, while daily maxima always exceeded 850 W m^{-2}. The average solar intensity di-
20 urnal profile maximum was 950 W m^{-2} at 12:00 (Fig. 4d). Wind speed was on average
4.6 m s^{-1} and no statistically significant diurnal pattern (at the 95% level) was observed
(Fig. 4c) during FAME-08, indicating no influence from land/sea breeze effects.

5.4 PM inorganic composition

PM$_1$ sulfate and ammonium measured by the Q-AMS. correlated well with those from
25 PM$_{1.3}$ filters ($R^2 = 0.95$ and 0.86 respectively). Nitrate did not correlate well because it
was associated mainly with NaNO$_3$ and with sizes above the AMS size cut-off. Nitrate

concentrations in the PM_1 fraction were low, typically below $0.1\,\mu g\,m^{-3}$ while in PM_{10} it was on average $3.9\,\mu g\,m^{-3}$.

Figure 5 shows the PM_1 sulfate, ammonium, nitrate and organics mass concentrations during the study. One-way ANOVA concluded that none of these species exhibited statistically significant diurnal variations (at the 95% level) indicating the lack of strong local aerosol sources.

Sulfate was the dominant constituent of PM_1 accounting for approximately half of the measured PM_1 mass (average concentration $4.7\,\mu g\,m^{-3}$) ranging from a minimum of $0.7\,\mu g\,m^{-3}$ to a maximum of $15.5\,\mu g\,m^{-3}$. Sulfate concentrations below $1.6\,\mu g\,m^{-3}$ were always associated with air masses of marine origin while concentrations above $10\,\mu g\,m^{-3}$ were associated with Athens, Greece and other continental sources. Ammonium, which was strongly correlated with sulfate ($R^2=0.9$ based both on filters and Q-AMS data), accounted for 16% of the average $PM_{1.3}$ mass (average concentration $1.3\,\mu g\,m^{-3}$). EC accounted for 2% of the average $PM_{1.3}$ mass and the rest of the inorganic species (e.g. nitrate, phosphate, sodium, potassium, calcium, magnesium and chloride) for 7%.

$PM_{1.3}$ and $PM_{1.3-10}$ inorganic composition based on filter measurements are presented in Fig. 6. The coarse ($PM_{1.3-10}$) fraction was dominated by crustal components (50%) and nitrate (16%). Sulfate, Na^+ and Cl^- contributed to the average coarse mass by approximately 10% each.

$PM_{1.3}$ accounted on average for 47% of the PM_{10} mass (Fig. 7), reaching 75% on 17 and 27 May. The minimum contribution (21%) was observed when air masses originating from Africa caused a three-day Saharan dust event which started on 19 May and ended on 21 May. During the event the PM_{10} calcium concentration increased significantly along with other trace metals.

During this study PM_{10} Na^+ and Mg^{2+} correlated well with each other ($R^2 = 0.76$), indicating a common origin. Previous studies (Mihalopoulos et al., 1997; Kouvarakis et al., 2002) have also reported similar correlations and have attributed both constituents mainly to sea salt. PM_{10} Cl^- and Na^+ correlated well ($R^2 = 0.87$) with an average

FAME-08

M. Pikridas et al.

◄◄ | ►►

◄ | ►

Back | Close

Full Screen / Esc

Cl$^-$/Na$^+$ mass ratio equal to 0.87. This ratio is lower by a factor of 2.1 than the typical seawater composition, indicating a deficit in Cl$^-$. This is due to the reactions of acids with sea salt that release hydrogen chloride (Seinfeld and Pandis, 2006) and is often observed in polluted coastal areas such as Finokalia (Mihalopoulos et al., 1997).

5   During this campaign ICP-MS-determined Al, Ca and Fe for PM$_{1.3-10}$ were found to correlate well with each other ($R^2 > 0.83$) indicating a common crustal origin (Sciare et al., 2005). Because ICP-MS did not provide measurements of Si and because our findings were similar to those of Sciare et al. (2005), we used their approach to determine the dust contribution, which is based on iron, instead of the sum of oxides algorithm

10   of Malm et al. (1994). The rest of the elements determined by ICP-MS were typically below 0.01 μg m^{-3} with the exception of Zn, which had an average concentration of 0.1 μg m^{-3}. ICP-MS analysis was not conducted for the PM$_1$ fraction as recent studies in the same area have indicated that the elemental concentrations of crustal origin in this size fraction are close to zero (Koulouri et al., 2008).

15 **5.5 Organic PM**

In order to convert OC to organic matter (OM), OC was multiplied by 2.2 based on the AMS analysis of Hildebrandt et al. (2010). This value is consistent with the suggestions of Turpin and Lim (2001) for aged aerosol. Q-AMS organics and filter PM$_1$ OM correlated well ($R^2 = 0.79$). OM represented 28% (average concentration 2.3 μg m^{-3}) of the

20   PM$_1$ mass on average. The ANOVA test revealed a lack of diurnal pattern of the total organic aerosol measured by the Q-AMS, yet the fraction of the total organic aerosol mass due to fragments at m/z 43 and m/z 44 exhibited diurnal patterns of similar phase (Hildebrandt et al., 2010). The mass fragment at m/z 44 mostly corresponds to the CO$_2^+$ ion and can be used as a measure of the extent of oxidation. A detailed

25   analysis of the organic aerosol measured by the AMS during FAME-08 is presented in Hildebrandt et al. (2010).

The water soluble fraction of the PM$_1$ organic content was on average 79.5±7.8%

(Fig. 8). This large percentage of water soluble carbon supports our hypothesis that organic PM at Finokalia was highly aged. Furthermore, Q-AMS data analysis concluded that m/z 44 contributed on average 18% to the total organic mass (Hildebrandt et al., 2010) which points to a highly oxidized organic aerosol, typical for highly aged air masses (Jimenez et al., 2009).

The PM_1 filter based OC/EC slope was equal to 5.4 (Fig. 9) for the study period, with the exception of May 19 to May 21 where the slope was equal to 2.8 due to the high EC concentrations in the African air mass. An OC/EC slope equal to 5.4 suggests that a significant fraction of the organic PM is secondary, while a value of 2.8 indicates that the secondary formation is limited (Cabada et al., 2004; Lim and Turpin, 2002). All of the organic aerosol was oxygenated (OOA) during that period; hydrocarbon-like organic aerosol (HOA) was not present in detectable amounts (Hildebrandt et al., 2010). These results suggest strongly that HOA was converted to OOA in the 6–36 h of transport from the source areas to Crete in the strongly oxidizing environment of Eastern Mediterranean during FAME-08. The OC/EC ratio correlates moderately ($R^2 = 0.2$) with daily average ozone, but a time lag between the ozone peak and the OC/EC ratio was observed (Fig. 10). Using a time lag of one day the correlation increased ($R^2 = 0.44$) suggesting that the oxidation of organics does not take place near the site but away from it. Similar findings have been reported for urban areas (Cabada et al., 2004).

5.6 PM water content

The particles during FAME-08 always contained water according to both the Q-AMS and the DAASS, even when RH was low. Similar hygroscopic behavior during summer months has been reported before for sulfate rich PM (Klystov et al., 2005).

5.7 PM size distribution

Average number, surface area and volume size distributions are presented in Fig. 11. The SMPS-measured average number distribution was centered at 90 nm, the surface

FAME-08

M. Pikridas et al.

area distribution at 245 nm and the volume distribution at approximately 300 nm. Diurnal profiles of number, surface area and volume distributions did not exhibit any trends, which is consistent with the lack of local sources of particles. The average total number concentration was $2690 \pm 1072\,\text{cm}^{-3}$ (Fig. 12). Particles below 50 nm did not contribute significantly to the number concentrations ($N_{10-50} = 337 \pm 296\,\text{cm}^{-3}$) contrary to larger fractions ($N_{50-100} = 1044 \pm 581\,\text{cm}^{-3}$, $N_{100-500} = 1309 \pm 590\,\text{cm}^{-3}$). Source region analysis concerning number concentration indicates higher contributions from Athens, Greece and other continental source regions than for air masses of marine and African origin. N_{10-50} was also influenced by nucleation and growth of particles. During FAME-08 six nucleation events took place, accompanied by growth of the particles to the Aitken mode.

5.8 Gaseous species

Daily average concentrations of SO_2 and HNO_3 never exceeded 220 and 400 ppt respectively (Fig. 13). SO_2 and HNO_3 levels were below the detection limit (20 ppt) for 109 and 13 of the 180 analyzed samples, accounting for 61% and 7% of the duration of the campaign, respectively. Their average concentrations were 81 ± 70 ppt for SO_2 and 178 ± 100 ppt for HNO_3, respectively. The low SO_2/sulfate ratio (<0.05) suggests that the conversion of SO_2 to sulfate is almost complete by the time that the air masses arrive at Crete from all source areas. Hildebrandt et al. (2010) estimated a maximum OH value of 1.6×10^7 molecules cm^{-3} which corresponds to a SO_2 consumption rate of 6.3% per hour in this environment. Several SO_2 plumes were observed with concentrations reaching levels above 1 ppb. Most of these plumes were associated with transport from coal-fired power plants in northwest Turkey (Canakkale area) and the Peloponnese (Megalopoli area).

6 Conclusions

A month of ambient particulate and gas phase sampling was conducted at a remote area in the Eastern Mediterranean in order to characterize the properties and temporal variability of PM. The lack of statistically significant diurnal variation in the bulk concentration of all constituents monitored by the Q-AMS and in the number concentrations suggests the absence of strong local sources. The coarse ($PM_{1.3-10}$) fraction was dominated by crustal matter (50%) and sea salt (24%). The dominant PM_1 constituents were sulfate and organics, accounting for 50% and 26% of the dry mass respectively. On average 80% of the PM_1 organic aerosol was water soluble and its OC/EC ratio was equal to 5.4, indicating that the organic aerosol content was mainly secondary and highly oxidized. This conclusion is supported by the Q-AMS analysis of the PM_1 organics presented by Hildebrandt et al. (2010) in a companion paper. The OC/EC ratio was found to correlate ($R^2 = 0.44$) moderately with the average ozone of the previous day.

Analysis of retroplumes obtained from a particle dispersion model in backward mode combined with statistical tests was conducted and five source regions were identified (Athens, Greece, other continental, Africa, marine). The hot and dry air masses originating from Africa resulted in an increase in temperature by 4°C and a decrease in relative humidity by 16% on average. Air masses from Africa were also associated with increased dust concentrations, increased aerosol absorption, increased concentrations of small air ion (<2 nm), lower ozone and a decrease of the OC/EC ratio by half. Source regions Athens, Greece and other continental were associated with higher sulfate, organic and number concentrations. Air masses of marine origin had the lowest concentrations for all PM_1 species.

References

Albrecht, B. A.: Aerosols, cloud microphysics, and fractional cloudiness, Science, 245, 1227–1230, 1989

An, W. J., Pathak, R. K., Lee, B. H., and Pandis, S. N.: Aerosol volatility measurement using an improved thermodenuder: Application to secondary organic aerosol, J. Aerosol Sci., 38, 305–314, 2007.

Bartzis, J. G., Andronopoulos, S., Kulmala, M., Larsen, B., Lazaridis, M., Lohse, C., Mirabel, P. and Pilinis, C.: The BOND Project: The Marseille and Athens Experimental Campaign. An Overview, J. of Aerosol Sci. (European Aerosol Conference Budapest, Hungary 6–10 September 2004), p. 1167, 2004.

Cabada, J. C., Pandis, S. N., Subramanian, R., Robinson, A. L., Polidori, A., and Turpin, B.: Estimating the secondary organic aerosol contribution to $PM_{2.5}$ using the EC tracer method, Aerosol Sci. Technol., 38(S1),140–155, 2004.

Cruz, C. N. and Pandis, S. N.: Deliquescence and hygroscopic growth of mixed inorganic-organic atmospheric aerosol, Environ. Sci. Technol., 34, 4313–4319, 2000.

Dick, W. D., Saxena, P., and McMurry, P. H.: Estimation of water uptake by organic compounds in submicron aerosols measured during the Southeastern Aerosol and Visibility Study, J. Geophys. Res., 105, 1471–1479, 2000.

Eleftheriadis, K., Colbeck, I., Housiadas, C., Lazaridis, M., Mihalopoulos, N., Mitsakou, C., Smolik, J., and Zdimal, V.: Size distribution, composition and origin of the submicron aerosol in the marine boundary layer during the eastern Mediterranean "SUB-AERO" experiment, Atmos. Environ., 40, 6245–6260, 2006.

Gerasopoulos, E., Kouvarakis, G., Babasakalis, P., Vrekoussis, M., Putaud, J. P., and Mihalopoulos, N.: Origin and variability of particulate matter (PM_{10}) mass concentrations over the Eastern Mediterranean, Atmos. Environ., 40, 4679–4690, 2006.

Hallquist, M., Wenger, J. C., Baltensperger, U., Rudich, Y., Simpson, D., Claeys, M., Dommen, J., Donahue, N. M., George, C., Goldstein, A. H., Hamilton, J. F., Herrmann, H., Hoffmann, T., Iinuma, Y., Jang, M., Jenkin, M., Jimenez, J. L., Kiendler-Scharr, A., Maenhaut, W., McFiggans, G., Mentel, Th. F., Monod, A., Prevot, A. S. H., Seinfeld, J. H., Surratt, J. D., Szmigielski, R., and Wildt, J.: The formation, properties and impact of secondary organic aerosol: current and emerging issues, Atmos. Chem. Phys., 9, 5155–5236, 2009, http://www.atmos-chem-phys.net/9/5155/2009/.

Hildebrandt, L., Engelhart, G. J., Mohr, C., Kostenidou, E., Lanz, V. A., Bougiatioti, A., DeCarlo, P. F., Prévôt, A. S. H., Baltensperger, U., Mihalopoulos, N., Donahue, N. M., and Pandis, S. N.: Aged organic aerosol in the Eastern Mediterranean: The Finokalia Aerosol Measurement Experiment-2008, Atmos. Chem. Phys. Discuss., 10, 1847–1900, 2010, http://www.atmos-chem-phys-discuss.net/10/1847/2010/.

Jayne, J. T., Leard, D. C., Zhang, X., Davidovits, P., Smith, K. A., Kolb, C. E., and Worsnop, D. R.: Development of an aerosol mass spectrometer for size and composition analysis of submicron particles, Aerosol Sci. Technol., 33, 49–70, 2000.

Jimenez, J. L., Jayne, J. T., Shi, Q., Kolb, C. E., Worsnop, D. R., Yourshaw, I., Seinfeld, J. H., Flagan, R. C., Zhang, X., Smith, K. A., Morris, J., and Davidovits, P.: Ambient aerosol sampling using the Aerodyne Aerosol Mass Spectrometer, J. Geophys. Res., 108 (D7), 8425, doi:10.1029/2001JD001213, 2003.

Jimenez, J. L., Canagaratna, M. R., Donahue, N. M., Prevot, A. S. H., Zhang, Q., Kroll, J. H., DeCarlo, P. F., Allan, J. D., Coe, H., Ng, N. L., Aiken, A. C., Docherty, K. D., Ulbrich, I. M., Grieshop, A. P., Robinson, A. L., Duplissy, J., Smith, J. D., Wilson, K. R., Lanz, V. A., Hueglin, C., Sun, Y. L., Tian, J., Laaksonen, A. T. R., Rautiainen, J., Vaattovaara, P., Ehn, M., Kulmala, M., Tomlinson, J. M., Collins, D. R., Cubison, M. J., Dunlea, E. J., Huffman, J. A., Onasch, T. B., Alfarra, M. R., Williams, P. I., Bower, K., Kondo, Y., Schneider, J., Drewnick, F., Borrmann, S., Weimer, S., Demerjian, K., Salcedo, D., Cottrell, L., Griffin, R., Takami, A., Miyoshi, T., Hatakeyama, S., Shimono, A., Sun, J. Y., Zhang, Y. M., Dzepina, K., Kimmel, J. R., Sueper, D., Jayne, J. T., Herndon, S. C., Trimborn, A. M., Williams, L. R., Wood, E. C., Kolb, C. E., Baltensperger, U., and Worsnop, D. R.: Evolution of organic aerosol in the atmosphere, Science, 326, 1525–1529, 2009.

Kalivitis, N., Gerasopoulos, E., Vrekoussis, M., Kouvarakis, G., Kubilay, N., Hatzianastassiou, N., Vardavas, I., and Mihalopoulos, N.: Dust transport over the eastern Mediterranean derived from Total Ozone Mapping Spectrometer, Aerosol Robotic Network, and surface measurements. J. Geophys. Res., 112, D03202, doi:10.1029/2006JD007510, 2007.

Kalivitis, N., Birmili, W., Stock, M., Wehner, B., Massling, A, Wiedensohler, A., Gerasopoulos, E., and Mihalopoulos, N.: Particle size distributions in the Eastern Mediterranean troposphere, Atmos. Chem. Phys., 8, 6729–6738, 2008, http://www.atmos-chem-phys.net/8/6729/2008/.

Kanakidou, M., Seinfeld, J. H., Pandis, S. N., Barnes, I., Dentener, F. J., Facchini, M. C., Van Dingenen, R., Ervens, B., Nenes, A., Nielsen, C. J., Swietlicki, E., Putaud, J. P., Balkanski,

Title Page

Abstract	Introduction
Conclusions	References
Tables	Figures

|◀ | ▶|

◀ | ▶

Back | Close

Full Screen / Esc

Printer-friendly Version

Interactive Discussion

Y., Fuzzi, S., Horth, J., Moortgat, G. K., Winterhalter, R., Myhre, C. E. L., Tsigaridis, K., Vignati, E., Stephanou, E. G., and Wilson, J.: Organic aerosol and global climate modelling: A review, Atmos. Chem. Phys., 5, 1053–1123, 2005, http://www.atmos-chem-phys.net/5/1053/2005/.

5 Kavouras, I. G. and Stephanou, E. G.: Particle size distribution of organic primary and secondary aerosol constituents in urban, background marine, and forest atmosphere, J. Geophys. Res., 107(D8), 4069, doi:10.1029/2000JD000278, 2002.

Khlystov, A., Wyers, G. P., and Slanina, J.: The steam-jet aerosol collector, Atmos. Environ., 29, 2229–2234, 1995.

10 Khlystov, A., Stanier, C. O., Takahama, S., and Pandis, S. N.: Water content of ambient aerosol during the Pittsburgh Air Quality Study, J. Geophys. Res., 110, D07S10, doi:10.1029/2004JD004651, 2005.

Kostenidou, E., Pathank, R. K., and Pandis, S. N.: An algorithm for the calculation of secondary organic aerosol density combining AMS and SMPS data, Aerosol Sci. Technol., 41, 1002–

15 1010, 2007

Koulouri, E., Saarikoski, S., Theodosi, C., Markaki, Z., Gerasopoulos, E., Kouvarakis, G., Makela, T., Hillamo, R., and Mihalopoulos, N.: Chemical composition and sources of fine and coarse aerosol particles in the Eastern Mediterranean, Atmos. Environ., 42, 6542–6550, 2008.

20 Kouvarakis, G., Tsigaridis, K., Kanakidou, M., and Mihalopoulos, N.: Temporal variations of surface regional background ozone over Crete Island in the Southeast Mediterranean, J. Geophys. Res., 105, 399–407, 2000.

Kouvarakis, G., Doukelis, Y., Mihalopoulos, N., Rapsomanikis, S., Sciare, J., and Blumthaler, M.: Chemical, physical, and optical characterization of aerosols during PAUR II experiment,

25 J. Geophys. Res., 107, 8141, doi:10.1029/2000JD000291, 2002.

Kulmala, M., Vehkamäki, H., Petäjä, T., Dal Maso, M., Lauri, A., Kerminen, V. M., Birmili, W., and McMurry, P. H.: Formation and growth rates of ultrafine atmospheric particles: a review of observations, J. Aerosol Sci., 35, 143–176. 2004.

Kulmala, M. and Kerminen, V. M.: On the formation and growth of atmospheric nanoparticles,

30 Atmos. Res., 90, 132–150, 2008.

Kulmala, M., Asmi, A., Lappalainen, H. K., Carslaw, K. S., Pöschl, U., Baltensperger, U., Hov, Ø., Brenquier, J.-L., Pandis, S. N., Facchini, M. C., Hansson, H.-C., Wiedensohler, A., and O'Dowd, C. D.: Introduction: European Integrated Project on Aerosol Cloud Climate and Air

FAME-08

M. Pikridas et al.

Quality interactions (EUCAARI) - integrating aerosol research from nano to global scales, Atmos. Chem. Phys., 9, 2825–2841, 2009, http://www.atmos-chem-phys.net/9/2825/2009/.

Lazaridis, M., Dzumbova, L., Kopanakis, I., Ondracek, J., Glytsos, T., Aleksandropoulou, V.,
Voulgarakis, A., Katsivela, E., Mihalopoulos, N., and Eleftheriadis, K.: PM_{10} and $PM_{2.5}$ levels in the Eastern Mediterranean (Akrotiri Research Station, Crete, Greece), Water Air Soil Pollut., 189, 85–101, 2008.

Lee, B. H., Kostenidou, E., Hildebrandt, L., Riipinen, I., Engelhart, G. J., Mihalopoulos, N., Prevot, A. S. H., Baltensperger, U., and Pandis, S. N.: Measurement of the ambient organic
aerosol volatility distribution: Application during the Finokalia Aerosol Measurement Experiment (FAME-2008), Atmos. Chem. Phys., in preparation, 2010.

Lim, H. and Turpin, B. J.: Origins of primary and secondary organic aerosol in Atlanta: Results of time-resolved measurements during the Atlanta Supersite Experiment. Environ. Sci. Technol., 36, 4489–4496, 2002.

Lohmann U. and Feichter J.: Global indirect aerosol effects: a review, Atmos. Chem. Phys., 5, 715–737, 2005, http://www.atmos-chem-phys.net/5/715/2005/.

Loo, B. W. and Cork, C. P.: Development of a high efficiency virtual impactor, Aerosol Sci. Technol., 9, 167–176, 1988.

Malm, W. C., Sisler, J. F., Huffman, D., Eldred, R. A., and Cahill, T. A.: Spatial and seasonal
trends in particle concentration and optical extinction in the United States, J. Geophys. Res., 99, 1347–1370, 1994.

Meyer, N. K., Duplissy, J., Gysel, M., Metzger, A., Dommen, J., Weingartner, E., Alfarra, M. R., Prevot, A. S. H., Fletcher, C., Good, N., McFiggans, G., Jonsson, A. M., Hallquist, M., Baltensperger, U., and Ristovski, Z. D.: Analysis of the hygroscopic and volatile properties of
ammonium sulphate seeded and unseeded SOA particles, Atmos. Chem. Phys., 9, 721–732, 2009, http://www.atmos-chem-phys.net/9/721/2009/.

Mihalopoulos, N., Stephanou, E., Kanakidou, M., Pilitsidis, S., and Bousquet, P.: Tropospheric aerosol ionic composition above the Eastern Mediterranean Area, Tellus B, 314–326, 1997.

Mirme, A., Tamm, E., Mordas, G., Vana, M., Uin, J., Mirme, S., Bernotas, T., Laakso, L., Hir-
sikko, A., and Kulmala, M.: A wide-range multi-channel Air Ion Spectrometer, Boreal Environ. Res., 12, 247–264, 2007.

Moulin, C., Lambert, C. E., Dayan, U., Masson, V., Ramonet, M., Bousquet, P., Legrand, M., Balkanski, Y. J., Guelle, W., Marticorena, B., Bergametti, G., and Dulac, F.: Satellite clima-

tology of African dust transport in the Mediterranean atmosphere, J. Geophys. Res., 103, 13137–13144, 1998.

Pope, C. A., Ezzati, M., and Dockery, D. W.: Fine-particulate air pollution and life expectancy in the United States, New Engl. J. Med. 360, 376–386, 2009.

5 Pope, C. A.: Respiratory hospital admission associated with PM_{10} pollution in Utah, Salt Lake and Cache Valleys, Arch Environ. Health, 7, 46–90, 1991.

Robinson, A. L., Donahue, N. M., Shrivastava, M. K., Weitkamp, E. A., Sage, A. M., Grieshop, A. P., Lane, T. E., Pierce, J. R., and Pandis, S. N.: Rethinking organic aerosols: Semivolatile emissions and photochemical aging, Science, 315, 1259–1262, 2007.

10 Saarikoski, S., Timonen, H., Saarnio, K., Aurela, M., Järvi, L., Keronen, P., Kerminen V. M., and Hillamo, R.: Sources of organic carbon in fine particulate matter in northern European urban air, Atmos. Chem. Phys. 8, 6281–6295, 2008.

Sciare, J., Bardouki, H., Moulin, C., and Mihalopoulos, N.: Aerosol sources and their contribution to the chemical composition of aerosols in the Eastern Mediterranean Sea during
15 summertime, Atmos. Chem. Phys., 3, 291–302, 2003a, http://www.atmos-chem-phys.net/3/291/2003/.

Sciare, J., Cachier, H., Oikonomou, K., Ausset, P., Sarda-Esteve, R., and Mihalopoulos, N.: Characterization of carbonaceous aerosols during the MINOS campaign in Crete, July–August 2001: a multi-analytical approach, Atmos. Chem. Phys., 3, 1743–1757, 2003b,
20 http://www.atmos-chem-phys.net/3/1743/2003/.

Sciare, J., Oikonomou, K., Cachier, H., Mihalopoulos, N., Andreae, M., O., Maenhaut, W., and Estève, R., S.: Aerosol mass closure and reconstruction of the light scattering coefficient over the Eastern Mediterranean Sea during the MINOS campaign, Atmos. Chem. Phys., 5, 2253–2265, 2005, http://www.atmos-chem-phys.net/5/2253/2005/.

25 Sciare, J., Oikonomou, K., Favez, O., Liakakou, E., Markaki, Z., Cachier, H., and Mihalopoulos, N.: Long-term measurements of carbonaceous aerosols in the Eastern Mediterranean: evidence of long-range transport of biomass burning, Atmos. Chem. Phys., 8, 5551–5563, 2008, http://www.atmos-chem-phys.net/8/5551/2008/.

Seibert, P. and Frank, A.: Source-receptor matrix calculation with a Lagrangian particle dis-
30 persion model in backward mode, Atmos. Chem. Phys., 4, 51–63, 2004, http://www.atmos-chem-phys.net/4/51/2004/.

Seinfeld, J. H. and Pandis, S. N.: Atmospheric Chemistry and Physics: from Air Pollution to Climate Change, John Wiley, New York, USA, 381–384, 1998.

FAME-08

M. Pikridas et al.

Title Page

Abstract	Introduction
Conclusions	References
Tables	Figures

|◄ | ►|

◄ | ►

Back | Close

Full Screen / Esc

Printer-friendly Version

Interactive Discussion

Schneider, J., Borrmann, S., Wollny, A. G., Blasner, M., Mihalopoulos, N., Oikonomou, K., Sciare, J., Teller, A., Levin, Z., and Worsnop, D. R.: Online mass spectrometric aerosol measurements during the MINOS campaign (Crete, August 2001), Atmos. Chem. Phys., 4, 65–80, 2004, http://www.atmos-chem-phys.net/4/65/2004/.

Stanier, C. O., Khlystov, A., and Pandis, S. N.: Nucleation events during the Pittsburgh Air Quality Study: Description and relation to key meteorological, gas-phase, and aerosol parameters. Aerosol Sci. Technol, 38(S1), 253–264, 2004a.

Stanier, C. O., Khlystov, A., Chan, R., Mandiro, M., and Pandis, S. N.: A method for the in-situ measurement of fine aerosol water content of ambient aerosols: the Dry-Ambient Aerosol Size Spectrometer (DAASS), Aerosol Sci. Technol., 38, Supplement 1, 215–228, 2004b.

Stohl, A., Forster, V., Frank, A., Seibert, P., and Wotawa, G.: Technical Note : The Lagrangian particle dispersion model FLEXPART version 6.2, Atmos. Chem. Phys., 5, 2461–2474, 2005, http://www.atmos-chem-phys.net/5/2461/2005/.

Schwartz, J., Dockery, D. W., and Neas L., M.: Is daily mortality associated specifically with fine particles?, J. Air Waste Manag. Assoc., 46, 927–939, 1996.

Turpin, B. J. and Lim, H. J.: Species contributions to PM2.5 mass concentrations: revisiting common assumptions for estimating organic mass, Aerosol Sci. Technol., 35, 602–610, 2001.

Twomey, S.: The influence of pollution on the shortwave cloud albedo of clouds, J. Atmos. Sci., 34, 1149–1154, 1977.

Wang, Z., Hopke, P. K., Ahmadi, G., Cheng, Y. S., and Baron, P. A.: Fibrous particle deposition in human nasal passage: The influence of particle length, flow rate, and geometry of nasal airway, J. Aerosol Sci., 39, 1040–1054, 2008.

Wheater C. P. and Cook, P. A.: Using Statistics to Understand the Environment, Routledge, New York, USA, 124–137, 2000.

Title Page

Abstract | Introduction

Conclusions | References

Tables | Figures

◄◄ | ►►

◄ | ►

Back | Close

Full Screen / Esc

Printer-friendly Version

Interactive Discussion

Table 1. Summary of FAME-08 measurements.

Variable	Instrument	Group	Resolution	Period of Operation
Aerosol Size Distribution				
Aerosol Number Distribution (10–500 nm)	TSI 3080 SMPS [a]	CAPS[b]	10 min	4 May–28 May
Aerosol Number Distribution (10–500 nm)	TSI 3034 SMPS[a]	U. of Aegean	3 min	8 May–8 June
Positive/Negative Ion Size Distribution (0.8–40 nm)	Air Ion Spectrometer	U. of Helsinki	5 min	4 May–8 June
Aerosol Chemical Composition				
Aerosol Water	DAASS[c]	CAPS[b]	10 min	4 May–28 May
PM_1 (non refractory) Size Resolved Composition	Q-AMS[d]	PSI[e] /CAPS[b]	3 min	8 May–7 June
Water Soluble Ions	Steam Sampler	U. of Patras	17 min	6 May–8 June
$PM_{1.3}$ and PM_{10} Inorganic Ions	Virtual Impactor with Ion Chromatography/ICP-MS[h]	ECPL[f]	Daily	4 May–8 June
PM_1 OC/EC	ECPL Sampler with Sunset Laboratories Carbon Analyzer	ECPL[f]	Daily	4 May–8 June
PM_1 WSOC	ECPL Sampler with Shimadzu TOC-Vcsh[i]	ECPL[f]	Daily	4 May–8 June
Aerosol Properties				
Light Scattering (wet/dry)	Radiance Research Integrating Nephelometer (Model M903)	ECPL[f]	5 min	4 May–7 June
Light Scattering (3 wavelengths)	Integrating Nephelometer (TSI Model 3563)	U. of Aegean	5 min	4 May–7 June
Organic Aerosol Volatility	Thermodenuder	CAPS[b]	20 min	8 May–7 June
Absorption	Magee Scientific Aethalometer (Model AE-20)	ECPL[f]	5 min	4 May–8 June
Absorption	PSAP (Particle Soot Absorption Photometer)	ECPL[f]	5 min	4 May–8 June
Gaseous Species				
O_3	Thermo electron Model 49C	ECPL[f]	5 min	4 May–7 June
O_3	Dasibi Model 1008 RS	ECPL[f]	5 min	4 May–7 June
CO	Thermo electron Model 48C	ECPL[f]	30 min	15 May–7 June
SO_2, HNO_3, HCl	Impregnated Glass Fiber Filters with IC analysis	ECPL[f]	6 h	4 May–6 June
NH_3	Impregnated Paper Filters with IC analysis	ECPL[f]	6 h	4 May–6 June
Meteorology				
Relative Humidity	MP101A Humidity-Temperature	ECPL[f]	5 min	4 May–8 June
Light intensity	Pyranometer CM3	ECPL[f]	5 min	4 May–8 June
Temperature	MP101A Humidity-Temperature	ECPL[f]	5 min	4 May–8 June
Wind Speed	05103 Wind Monitor	ECPL[f]	5 min	4 May–8 June
Wind Direction	05103 Wind Monitor	ECPL[f]	5 min	4 May–8 June

[a] SMPS: Scanning Mobility Particle Sizer; [b] CAPS: Center for Atmospheric Particle Studies at Carnegie Mellon University; [c] DAASS: Dry-Ambient Aerosol Size Spectrometer; [d] Q-AMS: Quadrupole Aerosol Mass Spectrometer; [e] PSI: Paul Scherrer Institut; [f] ECPL: Environmental Chemical Processes Laboratory (University of Crete); [g] IC: Ion chromatography; [i] TOC: Total Organic Carbon; [h] ICP-MS: CP-MS: Inductively Coupled Plasma Mass Spectrometry.

FAME-08

M. Pikridas et al.

Table 2. Source region analysis for meteorological, physical and chemical properties.

Variable	Instrument	Marine Average ±std	Number of values	North Africa Average ±std	Number of values	Athens Average ±std	Number of values	Greece Average ±std	Number of values	Continental Average ±std	Number of values
PM_1 Sulfate ($\mu g/m^3$)	Q-AMS	3.0±1.3	590	5.0±1.7	134	7.5±2.2	194	6.8±3.0	216	5.9±2.8	421
PM_1 Ammonium ($\mu g/m^3$)	Q-AMS	1.0±0.4	590	1.7±0.6	134	2.1±0.6	194	1.8±0.7	216	1.8±0.7	421
PM_1 Nitrate ($\mu g/m^3$)	Q-AMS	0.08±0.06	590	0.10±0.08	134	0.08±0.04	194	0.07±0.03	216	0.09±0.05	421
Acidity[1]	Q-AMS	0.89±0.19	590	0.90±0.12	134	0.75±0.08	194	0.75±0.11	216	0.83±0.12	421
PM_1 Organics ($\mu g/m^3$)	Q-AMS	2.1±0.8	590	1.9±0.8	134	3.2±0.9	194	2.6±0.7	216	3.2±1.0	421
Number Concentration (cm^{-3})	SMPS	2403±952	1825	2435±1075	167	3034±1043	324	3159±1197	448	3068±1037	812
Air Ions (<2 nm) (cm^{-3})	AIS	561±170	4452	662±225	684	511±1853	1056	487±146	1574	502±149	2436
Aerosol Absorption (Mm^{-1})	PSAP	4.6±1.7	4001	8.5±3.4	579	5.9±1.5	960	5.4±1.3	1290	5.9±1.7	2138
T (°C)	Rotronic	19.0±3.2	4594	24.8±3.1	684	19.6±3.4	1056	19.6±3.0	1581	19.2±3.9	2429
RH (%)	Rotronic	64.6±19.8	4575	46.5±22.4	682	61.6±20.1	961	60.7±19.3	1568	66.9±18.4	2365

[1] PM_1 acidity defined here as the ratio of ammonium to sulfate in molar equivalents as measured by the Q-AMS.

FAME-08

M. Pikridas et al.

Printer-friendly Version

Interactive Discussion
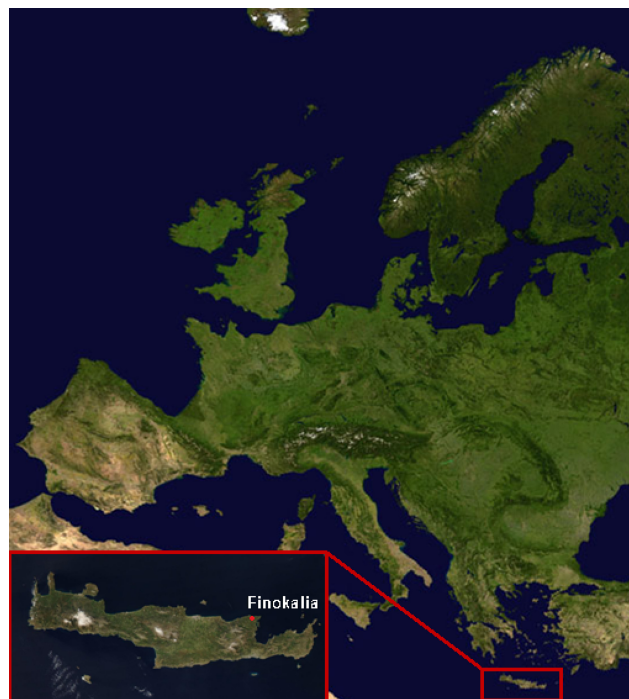
Fig. 1. NASA satellite images of Europe and of the island of Crete, indicating the location of the sampling station at Finokalia.
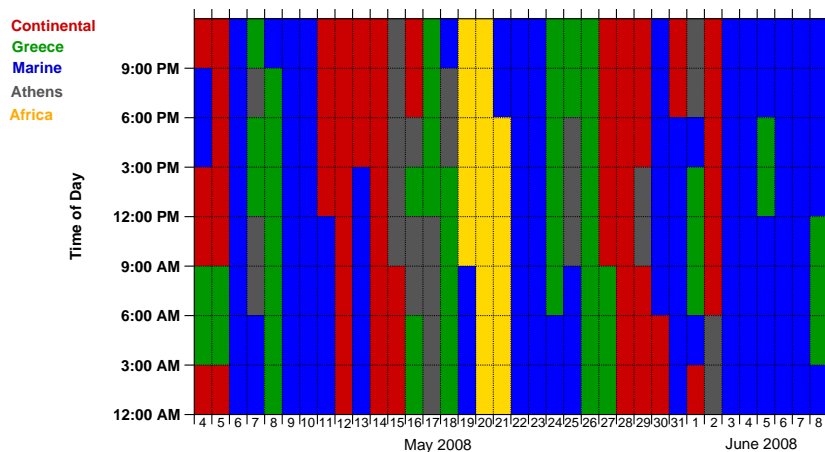
Fig. 2. Source region analysis based on FLEXPART footprint plots. Air masses were categorized based on their source region using PES of their footprint residence time plots (Stohl et al., 2005). A trajectory was attributed to a category if the source region had a PES value above 0.9 ns kg^{-1} in the corresponding footprint plot.
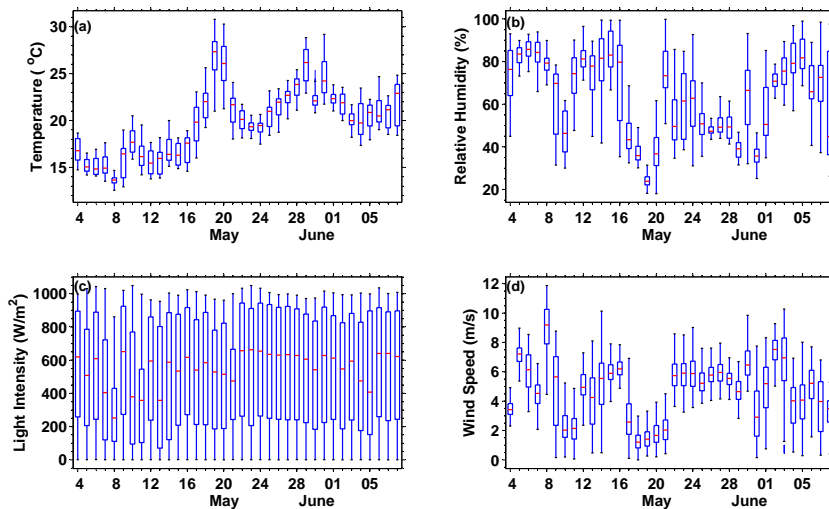
Fig. 3. Daily averages of ambient temperature **(a)**, relative humidity **(b)**, light intensity **(c)** and wind speed **(d)** during May 4 to June 8. Red lines indicate the median, boxes represent the upper and lower quartile and the whiskers extend to the most extreme data points. From 19 to 21 May (source region Africa) average daily temperature increased and relative humidity decreased.

M. Pikridas et al.
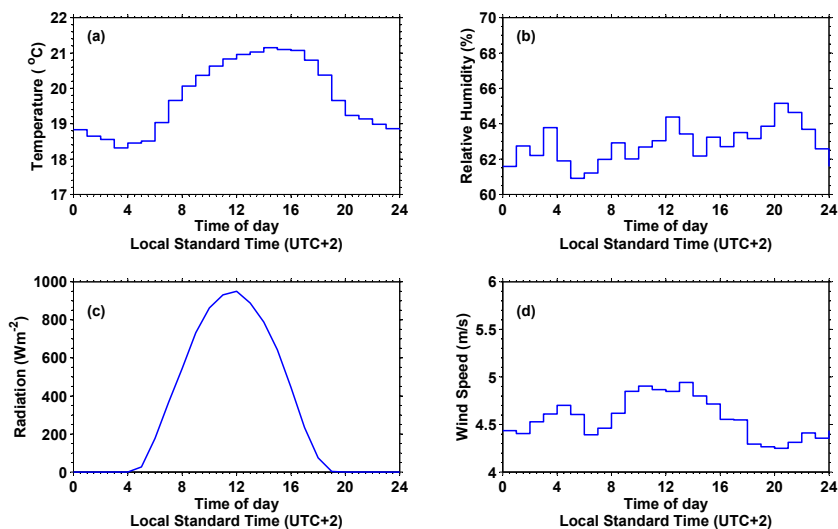
Fig. 4. Average diurnal variation in ambient temperature **(a)**, relative humidity **(b)**, light intensity **(c)** and wind speed **(d)**.
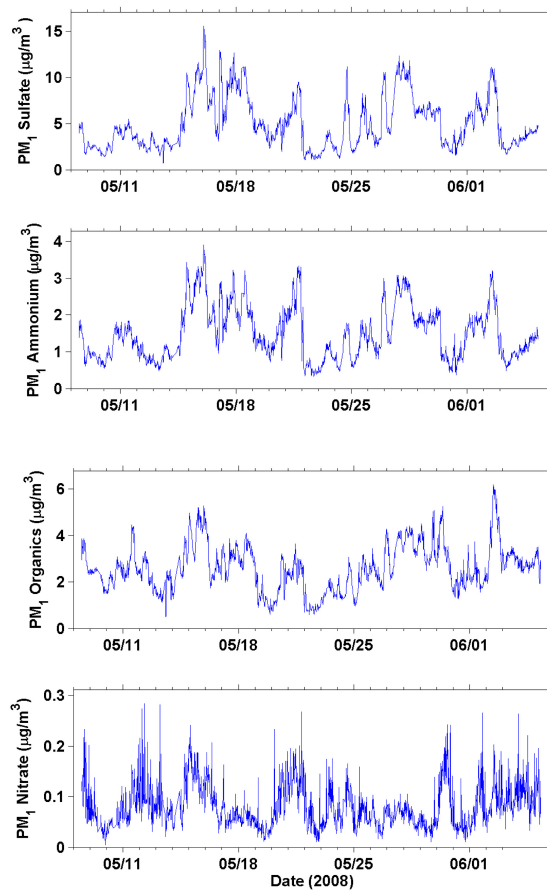
Fig. 5. Time series of PM$_1$ aerosol composition measured by the Q-AMS. Different scales are used for each graph.
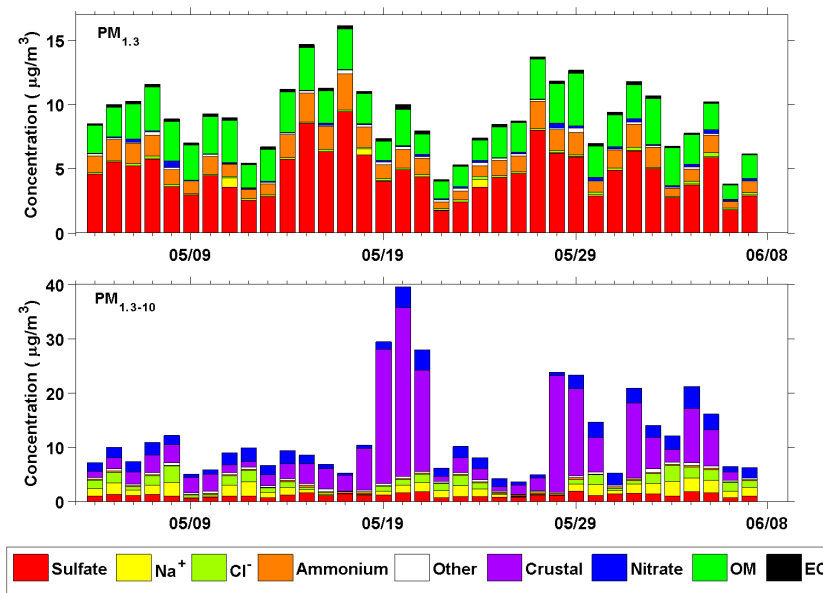
Fig. 6. Daily average of $PM_{1.3}$ and $PM_{1.3-10}$ during the study, based on filter measurements. OM was calculated as $OC^*2.2$ according to Hildebrandt et al. (2010). Crustal concentration is calculated using iron as a surrogate according to Sciare et al. (2005). Other is the sum of PO_4^{3-} and K^+.

FAME-08

M. Pikridas et al.
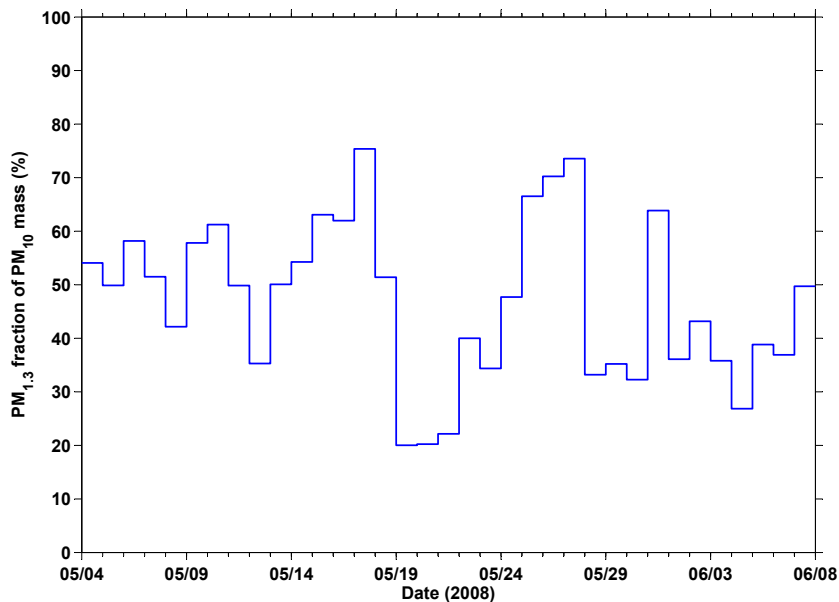
Fig. 7. Mass fraction of $PM_{1.3}$ over PM_{10} mass as a function of time.

FAME-08

M. Pikridas et al.

Printer-friendly Version

Interactive Discussion
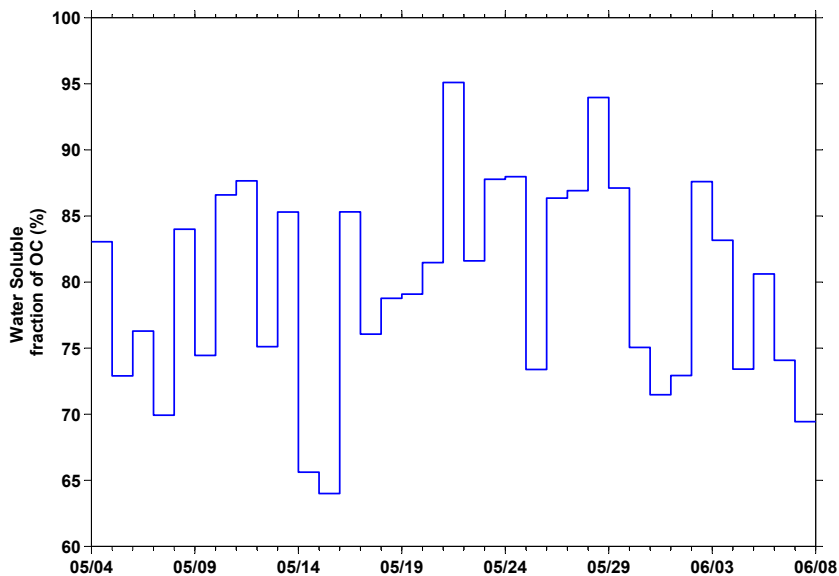
Fig. 8. Percentage of water soluble OC based on PM_1 filter measurements. On average 80% of OC was water soluble.
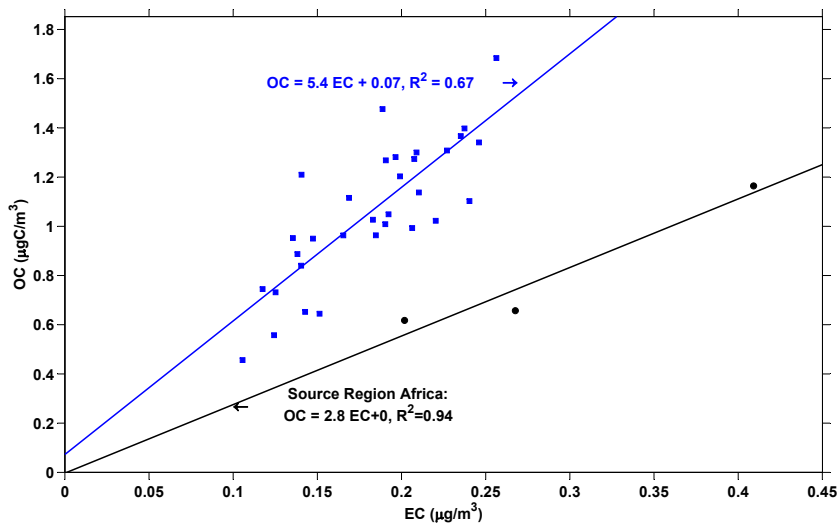
Fig. 9. OC versus EC as determined by PM_1 filters. The slope of the OC versus EC line was 5.4 (blue points) for the study period with the exception of 19 to 21 May (source region Africa), when it was equal to 2.8 (black points).
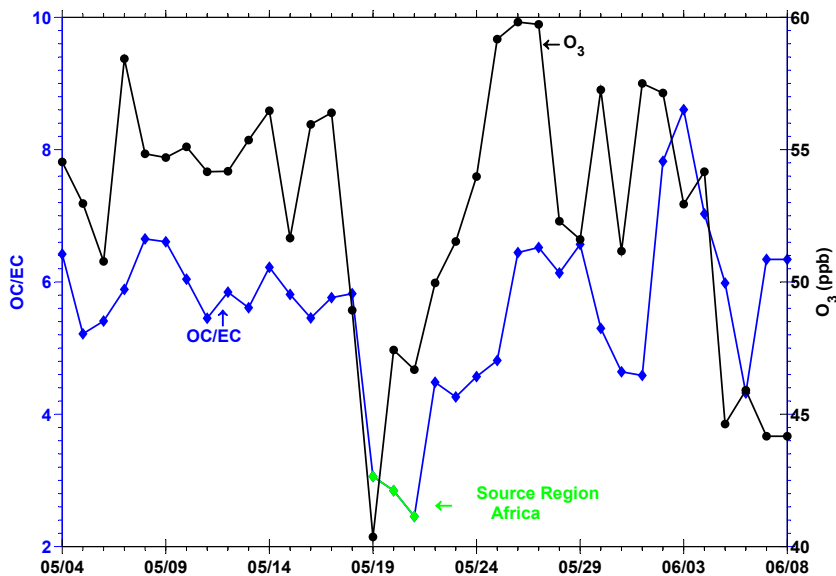
Fig. 10. OC/EC as a function of time. Ozone and OC/EC are moderately correlated and have a time lag of one day.

Printer-friendly Version

Interactive Discussion
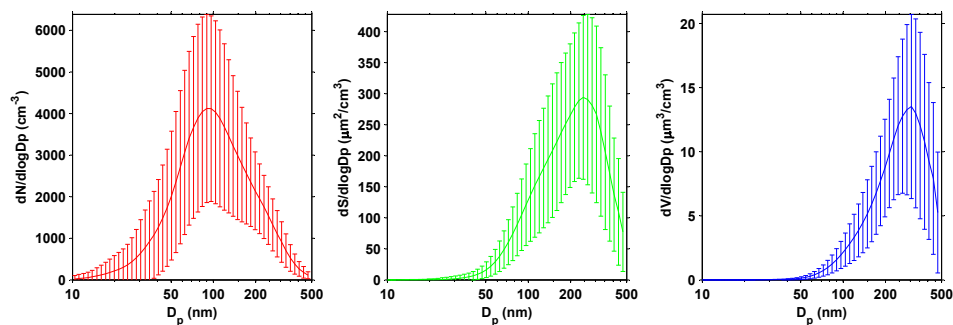
Fig. 11. Campaign average of number, surface area and volume distribution. Error bars represent one standard deviation from the average.
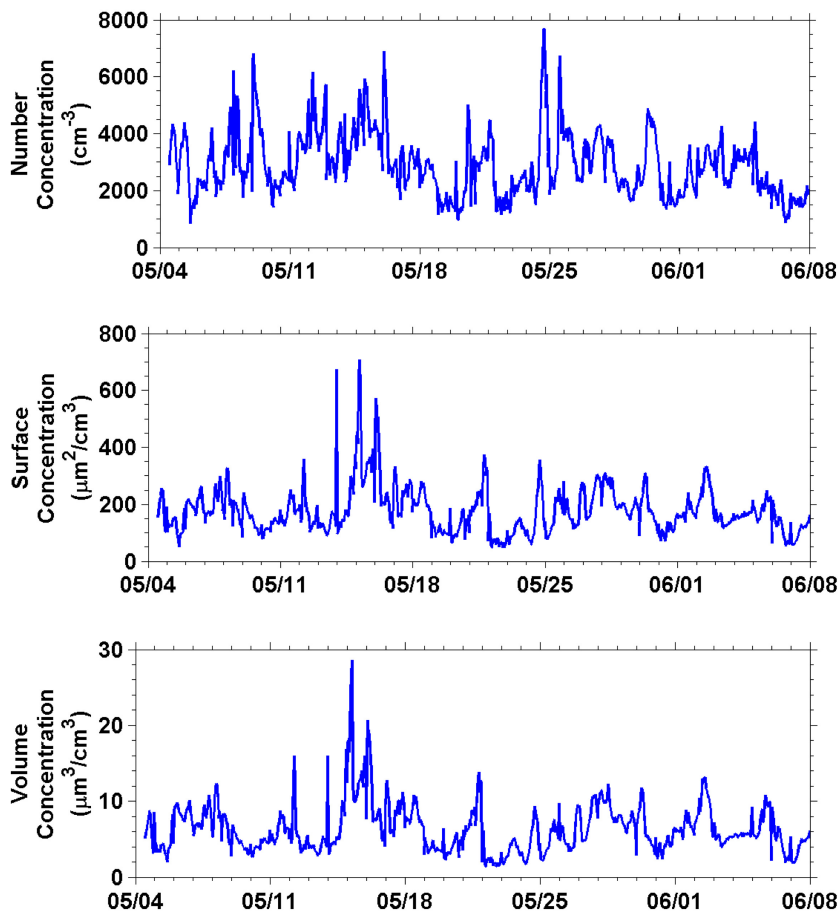
Fig. 12. Time series of number, surface area and volume concentrations for N_{10-500}.
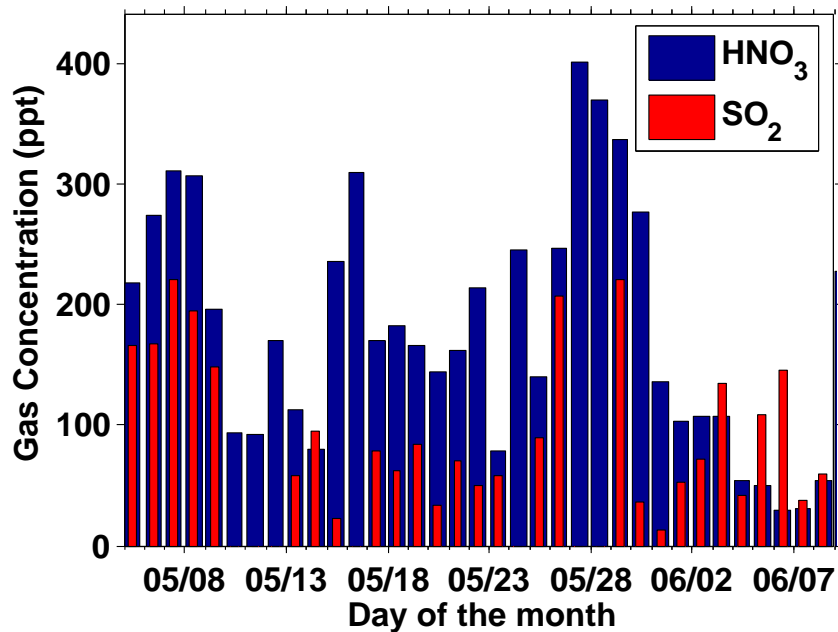
Fig. 13. Daily averages of acidic gaseous species (SO$_2$, HNO$_3$).